

# $\beta$ -NaYF<sub>4</sub>:Yb, Er at $\beta$ -NaYF<sub>4</sub> core/shell nanocrystals with significantly enhanced upconversion fluorescence by a successive two-step hot-injection approach

Qing Tian, Ke Tao, Kang Sun

State Key Laboratory of Metal Matrix Composites, School of Materials Science and Engineering, Shanghai Jiao Tong University, Shanghai 200240, People's Republic of China  
E-mail: ktao@sjtu.edu.cn

Published in Micro & Nano Letters; Received on 23rd June 2013; Revised on 13th August 2013; Accepted on 24th September 2013

Surface passivation is a general approach to enhance the luminescence of small-scaled size upconversion nanomaterials. In this reported work, a two-step hot-injection method was developed to synthesise core/shell structured NaYF<sub>4</sub>. A transmission electron microscope, X-ray diffraction and X-ray photoelectron spectroscopy were employed to prove the successful fabrication of  $\beta$ -NaYF<sub>4</sub>:Yb, Er at  $\beta$ -NaYF<sub>4</sub>. Core size and shell thickness were controlled by the amount of stabiliser and precursors addition, respectively. The upconversion efficiency of the resultant core/shell structured nanocrystals could be improved more than a 100-fold by comparison with the original core nanocrystals. Significant fluorescence enhancement was ascribed to the successive injection of precursors at elevated temperature.

**1. Introduction:** Upconversion nanoparticles (UCNPs) have generated extensive interest for their potential applications, especially in the biological field [1–4], owing to their advantages such as deep penetration in cells and tissues [5], no autofluorescence [6], no toxicity [7] and resistance to photobleaching [8]. Among various kinds of UCNPs, lanthanide (Ln) ions doped hexagonal phase ( $\beta$ ) NaYF<sub>4</sub> until now is acknowledged as the most efficient upconversion material mainly because of its low phonon energy host lattice [9, 10]. Different from their bulk counterparts, the doping ions in nanoscaled NaYF<sub>4</sub> particles are seriously affected by surface defects, ligand and solvent with high phonon energy. Therefore smaller UCNPs with higher surface-to-volume ratio show more multi-phonon relaxation and lower upconversion efficiency [11]. Many published references have reported that the fluorescence intensity of  $\beta$ -NaYF<sub>4</sub>:Yb, Er UCNPs decreased drastically with the reduction of crystal size [12–14]. Considering that UCNPs with < 30 nm size show obvious promise in biomedical applications as this size range is appropriate for cellular uptake and avoiding of body clearance [15], it is necessary to improve the luminescence efficiency of Ln doped NaYF<sub>4</sub> UCNPs with ultrasmall size.

Coating an NaYF<sub>4</sub> shell, as a surface passivation treatment, is a general and effective approach to improve the fluorescence efficiency of Ln doped NaYF<sub>4</sub> UCNPs. Up to now, several groups have successfully fabricated Ln doped  $\alpha$ -NaYF<sub>4</sub> at  $\alpha$ -NaYF<sub>4</sub> [16, 17],  $\beta$ -NaYF<sub>4</sub> at  $\alpha$ -NaYF<sub>4</sub> [18] and  $\beta$ -NaYF<sub>4</sub> at  $\beta$ -NaYF<sub>4</sub> [19–24]. As a best result, Yi and Chow [25] reported a 29.6 times increase of  $\beta$ -NaYF<sub>4</sub>:Yb, Tm after the growth of a  $\beta$ -NaYF<sub>4</sub> shell on its surface.

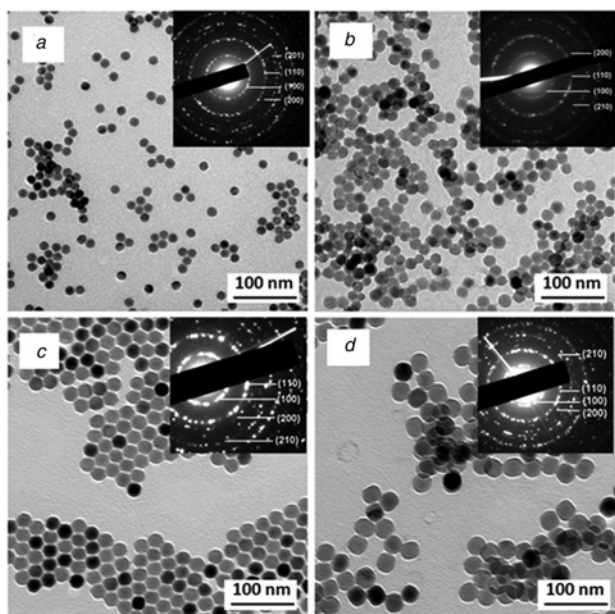
Our previous work showed a novel ‘hot-injection approach’ for the fabrication of  $\beta$ -NaYF<sub>4</sub>:Yb, Er nanocrystals with ultrasmall and controllable size [13, 14]. Here, two successive injections at an elevated temperature were performed to synthesise core/shell structured  $\beta$ -NaYF<sub>4</sub>:Yb, Er at  $\beta$ -NaYF<sub>4</sub> nanocrystals. We found that the fluorescence intensity can be improved over 100 times after the shell coating. Our results provide an efficient way to increase upconversion of nanocrystals’ fluorescent intensity, and may be helpful for understanding the mechanism on intensity improvement by coating a passive layer.

**2. Experimental:**  $\beta$ -NaYF<sub>4</sub>:Yb, Er UCNPs were synthesised by following our previous report with 1.89 mmol sodium oleate

(NaOL) and 2.16 mmol NaOL as stabiliser [14]. After the solution was maintained at 330°C for 10 min, a 10 ml solution was taken out for characterisation. Then, a shell precursor solution containing 1 mmol CF<sub>3</sub>COONa, 0.5 mmol (CF<sub>3</sub>COO)<sub>3</sub>Y, 4.7 ml oleic acid (OA), 5 ml octadecene and 0.945 mmol NaOL was injected drop by drop in 5 min. The reaction was continued for another 5 min. The solution was cooled down to room temperature and ethanol was added to precipitate the nanocrystals. The nanocrystals were washed with chloroform and methanol thrice to remove excess ligand.

Transmission electron microscope (TEM) images and selected area electron diffraction (SAED) patterns were obtained on a JEOL-JEM 2100 at an accelerating voltage of 200 kV. X-ray diffraction patterns were recorded with a Bruker-AXS X-ray diffractometer with Cu-K $\alpha$  radiation ( $\lambda = 0.15418$  nm). X-ray photoelectron spectroscopy (XPS) analysis was conducted on an AXIS Ultra<sup>DL</sup>. Upconversion fluorescence spectra were obtained on a Shimadzu RF5301PC luminescence spectrometer with an external 980 nm laser diode (1 W, continuous wave) as the excitation source in place of the xenon lamp in the spectrometer. Sample concentration was set as 10 mg/ml. The beam of a 980 nm laser was focused on a square spot with a size of 5 mm.

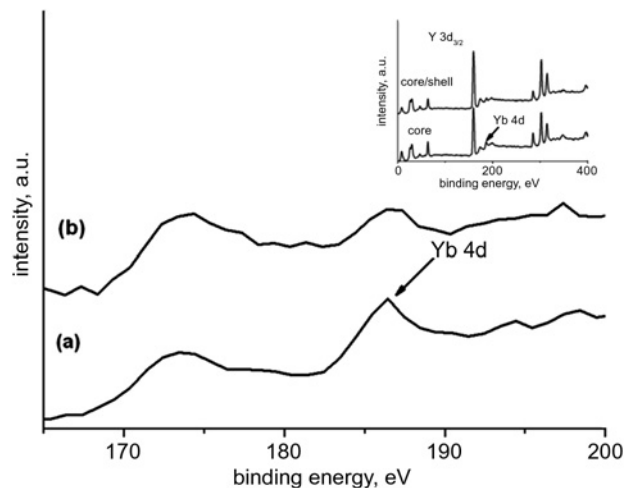
**3. Results and discussion:** Ultrasmall ( $13.7 \pm 1.0$  nm)  $\beta$ -NaYF<sub>4</sub>:Yb, Er UCNPs were synthesised following our previous report [14], as shown in Fig. 1a. A non-doped NaYF<sub>4</sub> shell was coated on the surface of the UCNPs by a consequent injection of precursors into the same spot at an elevated temperature. Fig. 1b shows the TEM image of the products after surface coating. The size of the nanocrystals increased to  $17.6 \pm 1.4$  nm while still remaining a spherical shape. The volume ratio of the shell to the core is about 1.12:1 ( $17.6^3/13.7^3 - 1$ ), which is near the molar ratio between the shell and the core precursors (1:1), indicating that all the shell precursors injected into the solvent grew on the core rather than nucleating separately. SAED patterns (Figs. 1a and b, inset) of the UCNPs before and after surface passivation match well with that of  $\beta$ -NaYF<sub>4</sub>, demonstrating that both the core and the shell products are pure hexagonal phase. The XRD patterns also confirmed this because all the diffraction peaks agree well with the calculated line of  $\beta$ -NaYF<sub>4</sub> (JCPDS file number PDF 16-0334), as shown in Fig. 1e. To further testify that our two-step hot-injection method can be applied to passivate



**Figure 1** TEM images of core  $\beta\text{-NaYF}_4\text{:Yb, Er}$  NPs with size of  $\sim 13.7$  nm (Fig. 1a) and  $\sim 22.0$  nm (Fig. 1c), and  $\beta\text{-NaYF}_4\text{:Yb, Er}$  at  $\beta\text{-NaYF}_4$  core/shell NPs, by using (a) as core (Fig. 1b) and (c) as core (Fig. 1d). XRD patterns of core and core/shell NPs corresponding to (a) and (b), respectively. Inset of a–d: SAED patterns of corresponding NPs

Ln doped  $\text{NaYF}_4$  nanocrystals with different size,  $22.0 \pm 1.2$  nm sized  $\beta\text{-NaYF}_4\text{:Yb, Er}$  nanocrystals were synthesised as the core. After coating, the size of the nanocrystals increased to  $28.0 \pm 2.1$  nm (Figs. 1c and d). Still, the volume ratio of the shell to the core is about 1.06, which is also near the ratio of the shell precursors to the core precursors utilised in the synthesis.

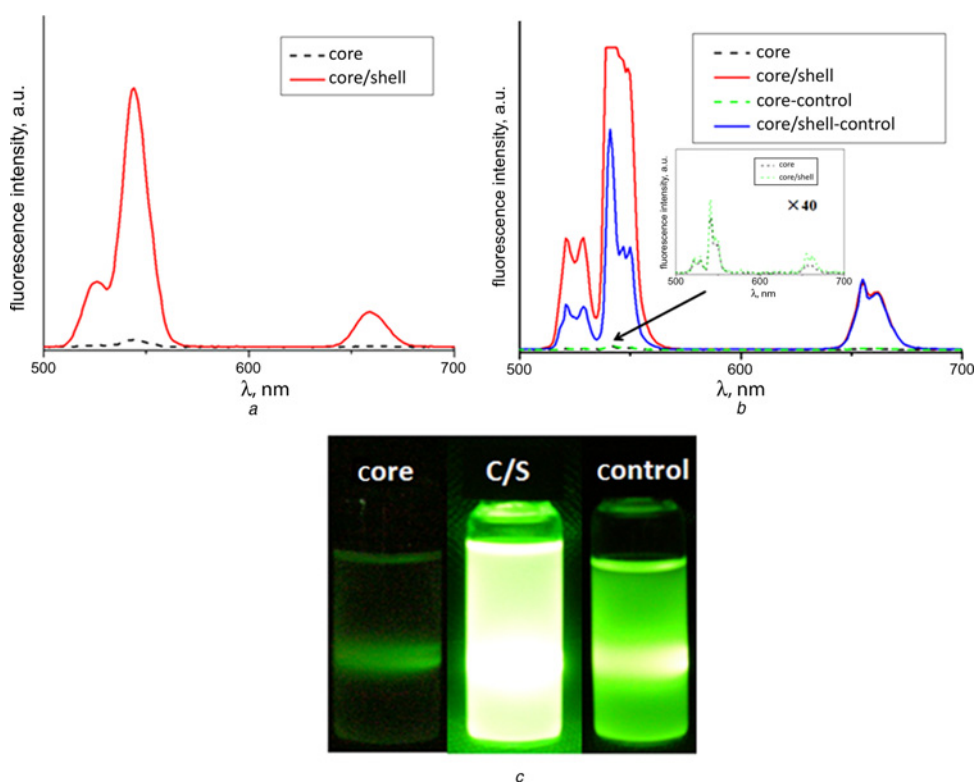
XPS analysis was performed to detect the element on the surface of the nanocrystals, for further confirming the successful coating. Fig. 2 shows the XPS spectrum of the core and core/shell products corresponding to the samples shown in Figs. 1a and b. Before coating (Fig. 2, trace (a)), a peak at 186.4 eV corresponding to the 4d electronic orbit of Yb in  $\beta\text{-NaYF}_4\text{:Yb, Er}$  core nanocrystals was detected. Although after surface passivation, the Yb 4d peak still appeared but weakened obviously, which means a shell without the Yb element has grown on the surface of the  $\beta\text{-NaYF}_4\text{:Yb, Er}$  nanocrystals. As the shell thickness is only 2.0 nm, the appearance of the Yb peak after coating is reasonable, which is also observed by Abel *et al.* [26] and Zhang and Zhang [17]. According to the above results, it can be concluded that core/shell structured  $\beta\text{-NaYF}_4\text{:Yb, Er}$  at  $\beta\text{-NaYF}_4$  was successfully synthesised with the two-step hot-injection method.



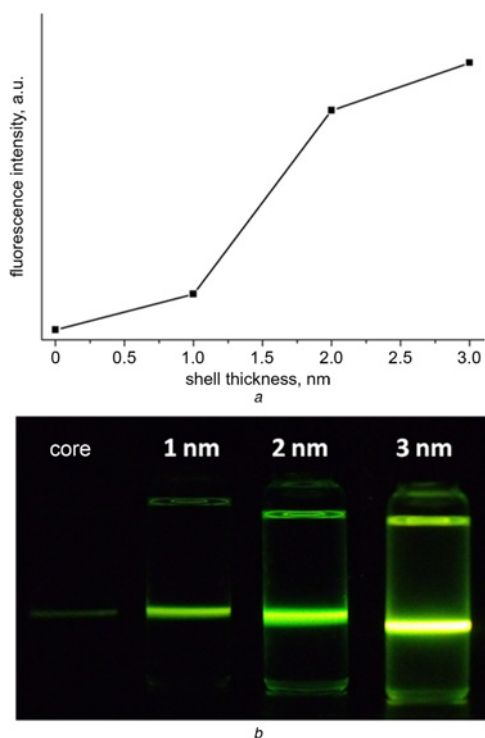
**Figure 2** XPS images (inset) and magnified XPS images of  $\beta\text{-NaYF}_4\text{:Yb, Er}$  NPs fabricated with 1.89 mmol NaOL (trace (a)) and  $\beta\text{-NaYF}_4\text{:Yb, Er}$  at  $\beta\text{-NaYF}_4$  core/shell NPs (trace (b))

Fig. 3 shows the fluorescence spectra of  $\beta\text{-NaYF}_4\text{:Yb, Er}$  and core/shell structured  $\beta\text{-NaYF}_4\text{:Yb, Er}$  at  $\beta\text{-NaYF}_4$ . After coating an  $\text{NaYF}_4$  layer, the fluorescence intensity was significantly enhanced for  $\sim 40.5$  and 107 times corresponding to 13.7 and 22.0 nm core nanocrystals, respectively. The shell thickness for the latter sample (Fig. 1d) about 3.0 nm is thicker than the former one (Fig. 1b, about 2.0 nm), resulting in the repair of the defects on the core nanocrystals' surface being more effective and multiphonon relaxation between the doping ions and ligand/solvent is suppressed [19]. Fig. 4 shows that the fluorescence intensity of the core/shell structured products is improved with the increase of the shell thickness, which is in accordance with Qian *et al.*'s report [19]. However, over 30 times fluorescence increase by surface coating is rarely reported [25]. The significant luminescence enhancement in the current work could be ascribed to the reasons as follows.

Firstly, 'hot-injection' at an elevated temperature favours the formation of a pure  $\beta\text{-NaYF}_4$  shell owing to the acceleration of the phase transition [13]. In Yi and Chow's paper [25],  $\alpha$  phase still exists in the shell according to their XRD results, which may hinder a further fluorescence improvement. Compared with the mixture of  $\alpha$  and  $\beta$  phase, the pure  $\beta\text{-NaYF}_4$  shell of our samples has lower phonon energy and less lattice mismatch on the interface of the core/shell, which favours effective fluorescence improvement. Furthermore, the growth of the  $\beta\text{-NaYF}_4$  shell happened immediately after the formation of  $\beta\text{-NaYF}_4\text{:Yb, Er}$  core nanocrystals under the same reaction environment, such as temperature and ligand content. Then, with our successive hot-injection method, the formation of the shell could also be recognised as a further growth of the core, which helps to reduce the defects on the interface of the core/shell. A control experiment with a non-successive two-step hot-injection approach was conducted to testify the above hypothesis, in which the reaction solution was cooled down to room temperature in 30 min and heated to 330°C again at a rate of  $20 \text{ K} \cdot \text{min}^{-1}$  before the shell precursor was injected. The core and core/shell products from this parallel experiment were denoted as core-control and core/shell-control, respectively, and their fluorescence spectra are shown in Fig. 3b. The fluorescence of the core product from a parallel experiment is similar to that of the core product from successive hot injections, whereas the core/shell product from the control experiment shows a much lower fluorescence intensity. The lower upconversion efficiency of the parallel coating experiment can also be observed by the naked eyes as shown in Fig. 3c. The size of the core and core-



**Figure 3** Fluorescence spectra of  $\sim 13.7$  nm  $\beta$ -NaYF<sub>4</sub>:Yb, Er core NPs, and its  $\beta$ -NaYF<sub>4</sub>:Yb, Er at  $\beta$ -NaYF<sub>4</sub> core/shell NPs (emission slit 5 nm) (Fig. 3a) and of  $\sim 22.0$  nm  $\beta$ -NaYF<sub>4</sub>:Yb, Er NPs, its  $\beta$ -NaYF<sub>4</sub>:Yb, Er at  $\beta$ -NaYF<sub>4</sub> core/shell NPs and the core and core/shell products from control experiment (emission slit 3 nm) (Fig. 3b). Photos of core, core/shell and core/shell-control products excited by 980 nm laser (Fig. 3c)



**Figure 4** Fluorescence intensity (Fig. 4a), and photos of  $\sim 13.7$  nm  $\beta$ -NaYF<sub>4</sub>:Yb, Er core NPs and its core/shell NPs with different shell thickness under 980 nm laser (Fig. 4b)

shell samples from the control experiment is  $22.4 \pm 1.2$  and  $27.9 \pm 2.2$  nm, respectively, as shown in Fig. 5. The sizes are similar to those of the successive hot-injection, indicating that the fluorescent intensity difference is not from the nanocrystals' size.

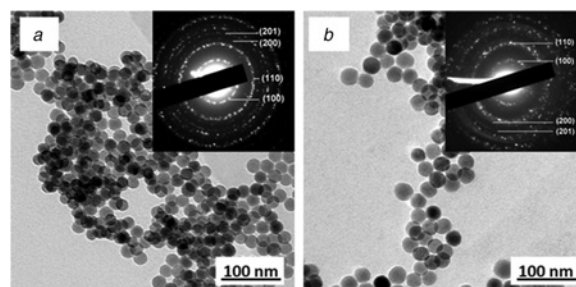


**Figure 5** TEM images of core (Fig. 5a) and core/shell (Fig. 5b) NPs from parallel experiment referring to samples shown in Fig. 3b

**4. Conclusion:** In summary,  $\beta$ -NaYF<sub>4</sub>:Yb, Er at  $\beta$ -NaYF<sub>4</sub> nanocrystals were successfully synthesised with a successive hot-injection approach. The fluorescence intensity of products with two different sizes was improved 40.5 and 107 times compared to the core nanocrystals, respectively. The significant fluorescence enhancement was ascribed to the successive injection of precursors at an elevated temperature.

**5. Acknowledgments:** This work was financially supported by the National Science Foundation of China (Project no. 31100718) and the Science and Technology Committee of Shanghai (Project no. 10520706500). The authors thank the Instrumental Analysis Center of SJTU for assistance with the instrumentation.

## 6 References

- [1] Wang F., Liu X.: 'Recent advances in the chemistry of lanthanide-doped upconversion nanocrystals', *Chem. Soc. Rev.*, 2009, **38**, (4), pp. 976–989

- [2] Ang L.Y., Lim M.E., Ong L.C., Zhang Y.: 'Applications of upconversion nanoparticles in imaging, detection and therapy', *Nanomedicine*, 2011, **6**, (7), pp. 1273–1288
- [3] He X., Wang K., Cheng Z.: 'In vivo near-infrared fluorescence imaging of cancer with nanoparticle-based probes', *Interdiscip. Rev., Nanomed. Nanobiotechnol.*, 2010, **2**, (4), pp. 349–366
- [4] Chatterjee D.K., Gnanasamandhan M.K., Zhang Y.: 'Small upconverting fluorescent nanoparticles for biomedical applications', *Small*, 2010, **6**, (24), pp. 2781–2795
- [5] Chatterjee D., Rufaihah A., Zhang Y.: 'Upconversion fluorescence imaging of cells and small animals using lanthanide doped nanocrystals', *Biomaterials*, 2008, **29**, (7), pp. 937–943
- [6] Tian Z., Chen G., Li X., *ET AL.*: 'Autofluorescence-free in vivo multi-color imaging using upconversion fluoride nanocrystals', *Lasers Med. Sci.*, 2009, **25**, (4), pp. 479–484
- [7] Shan J., Chen J., Meng J., *ET AL.*: 'Biofunctionalization, cytotoxicity, and cell uptake of lanthanide doped hydrophobically ligated NaYF<sub>4</sub> upconversion nanophosphors', *J. Appl. Phys.*, 2008, **104**, (9), p. 094308
- [8] Idris N.M., Li Z., Ye L., *ET AL.*: 'Tracking transplanted cells in live animal using upconversion fluorescent nanoparticles', *Biomaterials*, 2009, **30**, (28), pp. 5104–5113
- [9] Auzel F.: 'Materials and devices using double-pumped-phosphors with energy transfer', *Proc. IEEE*, 1973, **61**, (6), pp. 758–785
- [10] Auzel F.: 'Upconversion and anti-Stokes processes with f and d ions in solids', *Chem. Rev.*, 2004, **104**, (1), pp. 139–171
- [11] Suyver J.F., Aebischer A., Biner D., *ET AL.*: 'Novel materials doped with trivalent lanthanides and transition metal ions showing near-infrared to visible photon upconversion', *Opt. Mater.*, 2005, **27**, (6), pp. 1111–1130
- [12] Shan J., Ju Y.: 'A single-step synthesis and the kinetic mechanism for monodisperse and hexagonal-phase NaYF<sub>4</sub>:Yb, Er upconversion nanophosphors', *Nanotechnology*, 2009, **20**, (27), p. 275603
- [13] Tian Q., Tao K., Li W., Sun K.: 'Hot-injection approach for two-stage formed hexagonal NaYF<sub>4</sub>:Yb, Er nanocrystals', *J. Phys. Chem. C*, 2011, **115**, pp. 22886–22892
- [14] Sui Y., Tao K., Tian Q., Sun K.: 'Interaction between Y<sup>3+</sup> and oleate ions for the cubic-to-hexagonal phase transformation of NaYF<sub>4</sub> nanocrystals', *J. Phys. Chem. C*, 2012, **116**, (2), pp. 1732–1739
- [15] Longmire M., Choyke P.L., Kobayashi H.: 'Clearance properties of nano-sized particles and molecules as imaging agents: considerations and caveats', *Nanomedicine*, 2008, **3**, (5), pp. 703–717
- [16] Li X., Shen D., Yang J., *ET AL.*: 'Successive layer-by-layer strategy for multi-shell epitaxial growth: shell thickness and doping position dependence in upconverting optical properties', *Chem. Mater.*, 2013, **25**, (1), pp. 106–112
- [17] Zhang Q., Zhang Q.-M.: 'Synthesis and photoluminescent properties of  $\alpha$ -NaYF<sub>4</sub>:Nd/ $\alpha$ -NaYF<sub>4</sub> core/shell nanostructure with enhanced near infrared (NIR) emission', *Mater. Lett.*, 2009, **63**, (3–4), pp. 376–378
- [18] Mai H.X., Zhang Y.W., Sun L.D., Yan C.H.: 'Highly efficient multicolor up-conversion emissions and their mechanisms of monodisperse NaYF<sub>4</sub>:Yb, Er core and core/shell-structured nanocrystals', *J. Phys. Chem. C*, 2007, **111**, (37), pp. 13721–13729
- [19] Qian L.P., Yuan D., Shun Yi G., Chow G.M.: 'Critical shell thickness and emission enhancement of NaYF<sub>4</sub>: Yb, Er/NaYF<sub>4</sub>/silica core/shell/shell nanoparticles', *J. Mater. Res*, 2009, **24**, (12), pp. 3559–3568
- [20] Wang Y., Tu L., Zhao J., Sun Y., Kong X., Zhang H.: 'Upconversion luminescence of  $\beta$ -NaYF<sub>4</sub>: Yb<sup>3+</sup>, Er<sup>3+</sup>@ $\beta$ -NaYF<sub>4</sub> core/shell nanoparticles: excitation power density and surface dependence', *J. Phys. Chem. C*, 2009, **113**, (17), pp. 7164–7169
- [21] Qian H.-S., Zhang Y.: 'Synthesis of hexagonal-phase core-shell NaYF<sub>4</sub> nanocrystals with tunable upconversion fluorescence', *Langmuir*, 2008, **24**, (21), pp. 12123–12125
- [22] Qian L.P., Zhou L.H., Too H.-P., Chow G.-M.: 'Gold decorated NaYF<sub>4</sub>:Yb, Er/NaYF<sub>4</sub>/silica (core/shell/shell) upconversion nanoparticles for photothermal destruction of BE(2)-C neuroblastoma cells', *J. Nanoparticle Res.*, 2010, **13**, (2), pp. 499–510
- [23] Luo X., Akimoto K.: 'Upconversion properties in hexagonal-phase NaYF<sub>4</sub>:Er<sup>3+</sup>/NaYF<sub>4</sub> nanocrystals by off-resonant excitation', *Appl. Surface Sci.*, 2013, **273**, pp. 257–260
- [24] Dou Q., Idris N.M., Zhang Y.: 'Sandwich-structured upconversion nanoparticles with tunable color for multiplexed cell labeling', *Biomaterials*, 2013, **34**, (6), pp. 1722–1731
- [25] Yi G.-S., Chow G.-M.: 'Water-soluble NaYF<sub>4</sub>:Yb, Er(Tm)/NaYF<sub>4</sub>/polymer core/shell/shell nanoparticles with significant enhancement of upconversion fluorescence', *Chem. Mater.*, 2007, **19**, (3), pp. 341–343
- [26] Abel K.A., Boyer J.-C., Veggel F.C.J.M.: 'Hard proof of the NaYF<sub>4</sub>/NaGdF<sub>4</sub> nanocrystal core/shell structure', *J. Am. Chem. Soc.*, 2009, **131**, (41), pp. 14644–14645